Supplementary Information

Revealing Effect of Interfacial Electron Transfer in Heterostructured Co_9S_8@NiFe LDH for Enhanced Electrocatalytic Oxygen Evolution

Xueting Feng,[a, d] Qingze Jiao,[a, c] Zheng Dai,[a] Yanliu Dang,[e] Steven L. Suib,[d, e] Jiatao Zhang,[a] Yun Zhao,[a] Hansheng Li,[a] Caihong Feng[a, *] Anran Li[b, *]

[a] Beijing Key Laboratory for Chemical Power Source and Green Catalysis, School of Chemistry and Chemical Engineering, Beijing Institute of Technology, Beijing 100081, People's Republic of China

[b] Beijing Advanced Innovation Center for Big Data-Based Precision Medicine, School of Engineering Medicine, Beihang University, Beijing 100191, People's Republic of China

[c] School of Materials and Environment, Beijing Institute of Technology, Jinfeng Road No.6, Xiangzhou District, Zhuhai 519085, People's Republic of China

[d] Department of Chemistry, University of Connecticut, U-3060, 55 N. Eagleville Road, Storrs, Connecticut 06269, United States

[e] Institute of Materials Science, University of Connecticut, U-3136, 97 N. Eagleville Road, Storrs, Connecticut 06269, United States.

Corresponding Author

*Email: fengch@bit.edu.cn (Caihong Feng)

*Email: rananli@buaa.edu.cn (Anran Li)

EXPERIMENTAL SECTION

Materials. Cobalt sulfate heptahydrate ($CoSO_4•7H_2O$), Iron nitrate nonahydrate ($Fe(NO_3)_3•9H_2O$), Nickel(II) nitrate hexahydrate ($Ni(NO_3)_2•6H_2O$), thiourea (CH_4N_2S), urea, ethylene glycol (EG) and N,N-dimethylformamide (DMF) were purchased from Beijing Chemical Reagent Company. Nafion (5 wt%) were purchased from Alfa Aesar. All chemicals were analytical grade and used without further purification.

Preparation of the catalyst ink: 4 mg of the samples, 0.5 mg of super P and 30 μL of Nafion solution (5 wt%) were dispersed into 970 μL of 1:1 v/v isopropanol/water and sonicated for 1 h. The catalyst ink (10 μL) was deposited on a GC electrode, resulting in a mass loading of 0.2 mg/cm^2. The contrastive samples, including Co_9S_8, NiFe LDH and commercial IrO_2, were also investigated using the same mass loading.

Calculation of the Theoretical OER Activity: The overall OER process includes four elementary steps:

$$OH^- + * \rightarrow *OH + e^-$$

$$*OH + OH^- \rightarrow *O + H_2O + e^-$$

$$*O + OH^- \rightarrow *OOH + e^-$$

$$*OOH + OH^- \rightarrow * + O_2 + H_2O + e^-$$

where * and X* represent an adsorption site and an adsorbed X intermediate on the surface, respectively. Since calculating the thermochemistry of the OER under acidic condition is more convenient, the following elementary steps proposed by Nørskov et al. are considered, which are equivalent to the reactions shown above:[1-3]

$$H_2O + * \rightarrow HO* + H^+ + e^-$$

$$HO* + H_2O \rightarrow O* + H_2O + H^+ + e^-$$

$$O* + H_2O \rightarrow HOO* + H^+ + e^-$$

$$HOO* \rightarrow * + O_2 + H^+ + e^-$$

The free energy of $H^+ + e^-$ can be calculated as half of the formation energy of H_2 at 298 K and 1 atm. The free energy of the OER is computed by $\Delta G = \Delta E + \Delta ZPE - T\Delta S$, where ΔE can be obtained by the computation of geometrical structures, and ΔZPE and ΔS can be determined by computing vibrational frequencies and standards tables for the reactants and products in the gas phase.[4,5] Therefore, the Gibbs free energy changes of each step can be computed based on the following equations:

$$\Delta G_1 = E(HO*) - E(*) - E_{H2O} + 1/2E_{H2} + (\Delta ZPE - T\Delta S)_1 - eU$$

$$\Delta G_2 = E(O*) - E(HO*) + 1/2E_{H2} + (\Delta ZPE - T\Delta S)_2 - eU$$

$$\Delta G_3 = E(HOO*) - E(O*) - E_{H2O} + 1/2E_{H2} + (\Delta ZPE - T\Delta S)_3 - eU$$

$$\Delta G_4 = E(*) - E(HOO*) + E_{O2} + 1/2E_{H2} + (\Delta ZPE - T\Delta S)_4 - eU$$

Here, –eU term is included in the computation of reaction free energy, representing the applied external bias U.

Hu et al. found that the Fe sites had TOFs 20-200 times higher than the Ni sites such that at an Fe content of 4.7% and above the Fe sites dominate the catalysis.[6] They also showed that the OER catalytic activity of Ni-containing oxides upon Fe incorporation is dramatically increased due to the creation of a highly reactive surface active site, mostly likely based on Fe.[7] However, some works shows that the OER activity for $M^{2+\delta}O^{\delta}(OH)_{2-\delta}$/Pt(111) catalyst (M=Ni, Co, Fe, Mn) follows the order

Ni>Co>Fe>Mn.[8] In our work, the theoretical Fe content was more than 4.7%, and thus Fe sites were selected for the investigation of the OER processes in the DFT model.

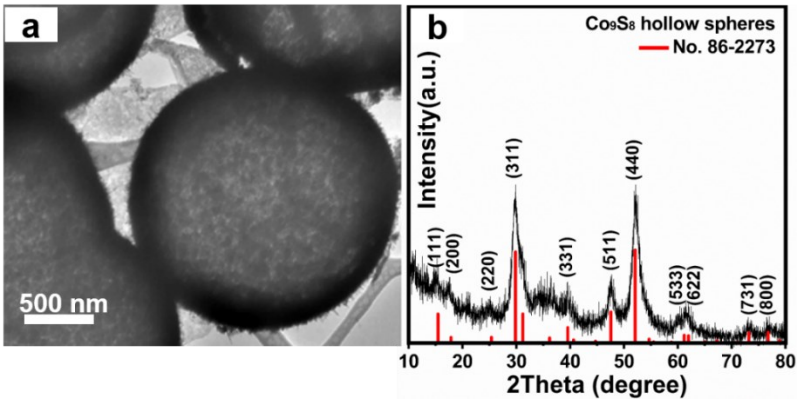

Fig. S1. (a) TEM image and (b) XRD pattern of Co_9S_8 hollow spheres.

The TEM image shows the Co_9S_8 hollow spheres with a diameter of ~2 μm consisted of numerous randomly assembled primary nanoparticles. The XRD pattern confirmed the component of pure Co_9S_8 (JCPDS No. 86-2273).

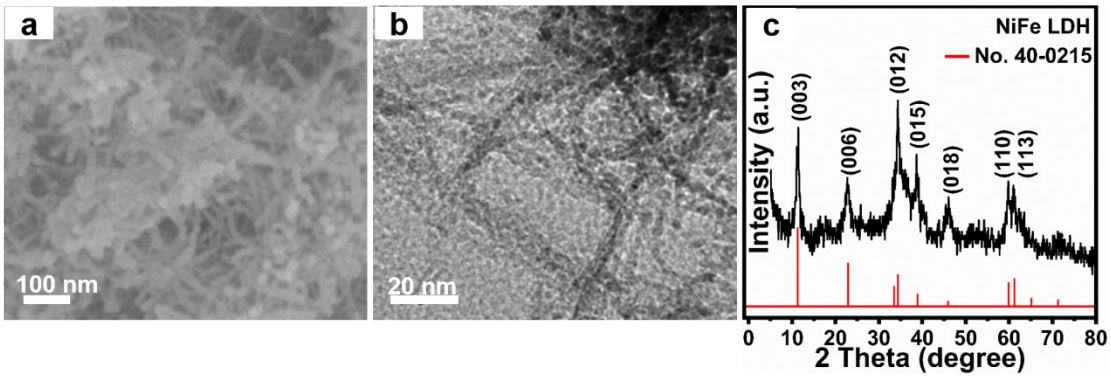

Fig. S2. (a) SEM image, (b) TEM image and (c) XRD pattern of NiFe LDH nanowires.

The SEM image in Fig. S2a shows that the NiFe LDH is composed of random interconnected nanowires that are inclined to aggregate. TEM is performed to further observe the detailed structure and morphology of NiFe LDH. As shown in Fig. S2b, each individual nanowire is assembled from numerous connected particles. The XRD pattern confirmed the component of pure NiFe LDH (JCPDS No. 40-0215).

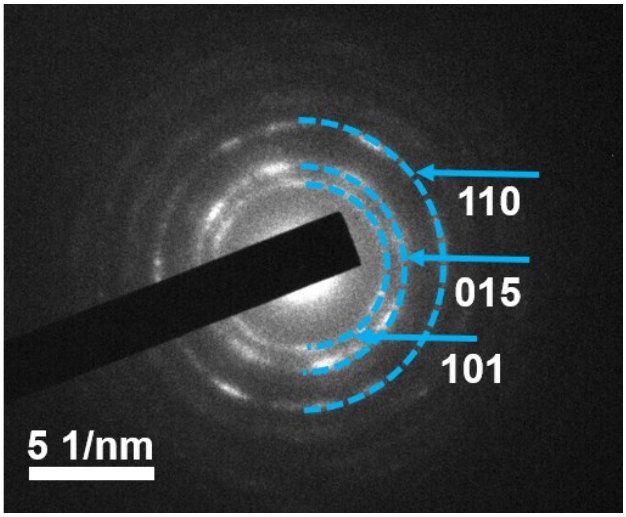

Fig. S3. SAED of NiFe LDH nanowires in the Co_9S_8@NiFe LDH.

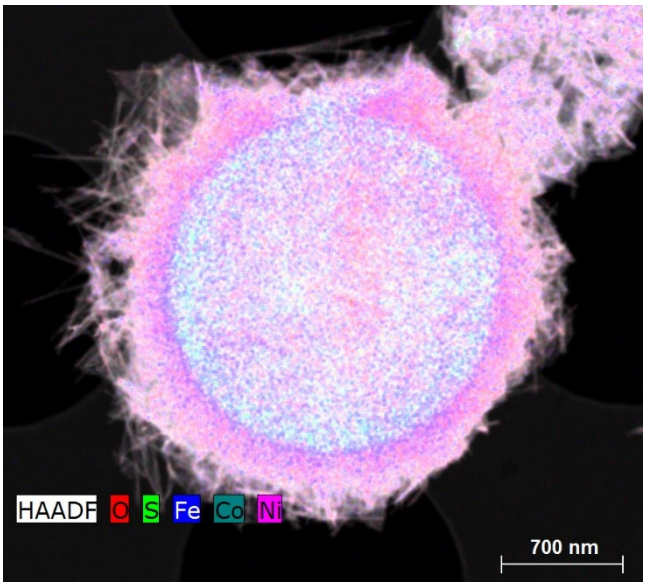

Fig. S4. EDS mapping for Co, Ni, Fe, S and O of Co_9S_8@NiFe LDH.

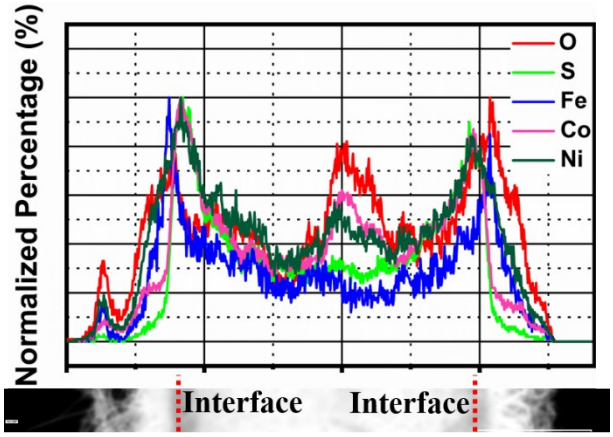

Fig. S5. EDS line scan of Co_9S_8@NiFe LDH.

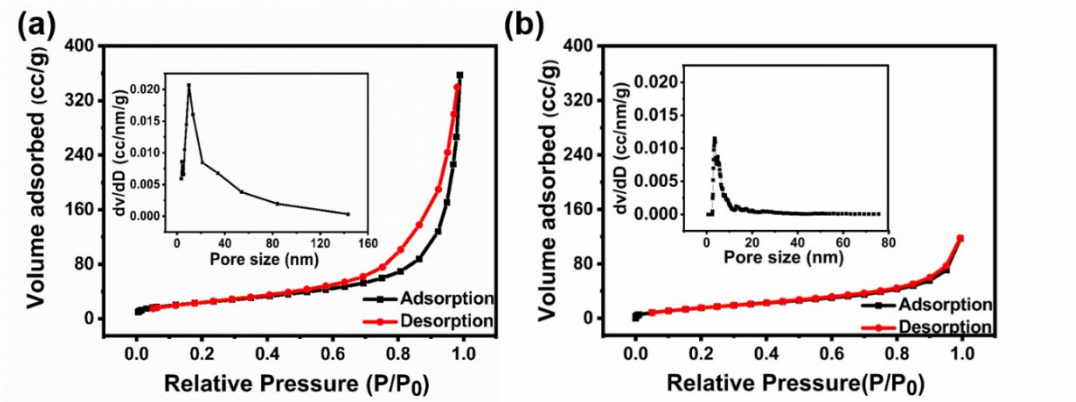

Fig. S6. N_2 adsorption-desorption isotherms and corresponding pore size distribution curves of (a) Co_9S_8@NiFe LDH and (b) Co_9S_8.

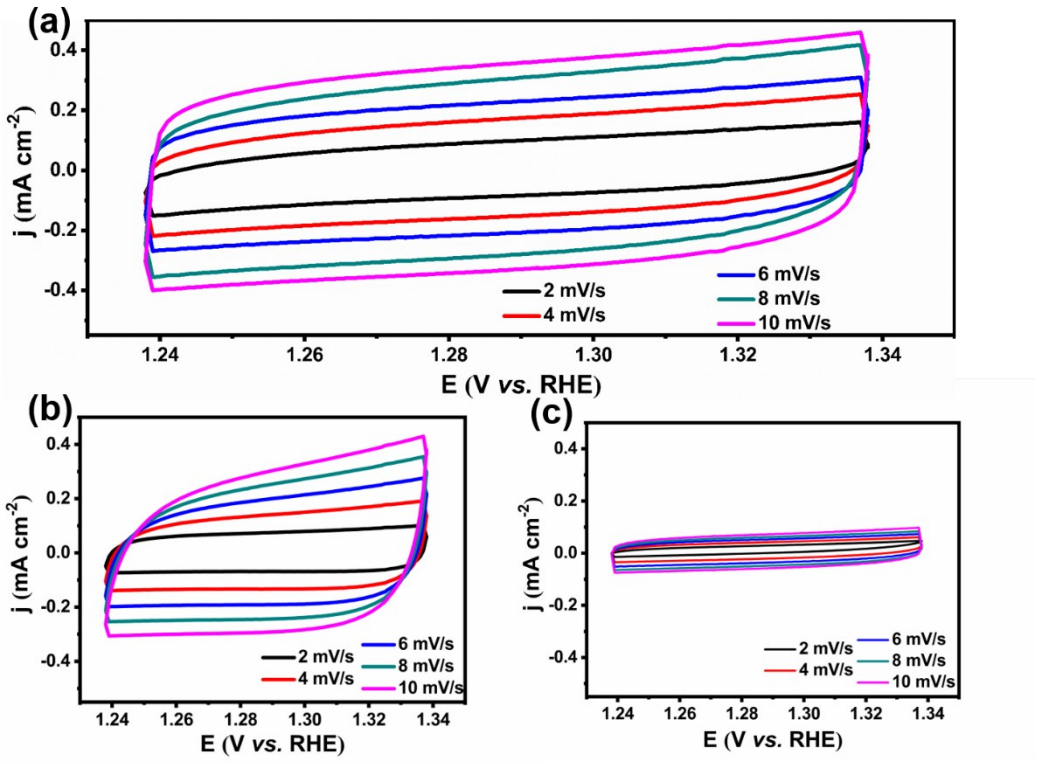

Fig. S7. CV measurement with various scan rates for (a) Co_9S_8@NiFe LDH, (b) Co_9S_8 and (c) NiFe LDH in 1 M KOH.

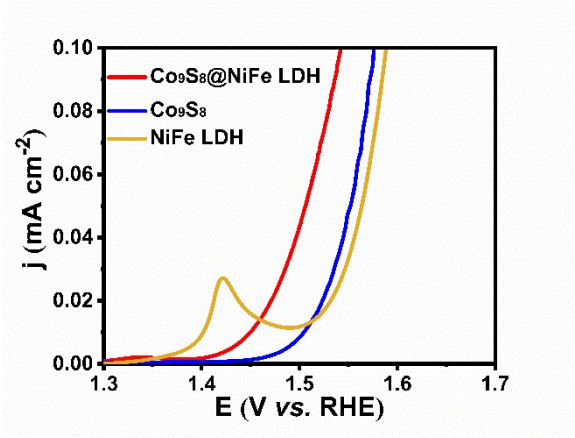

Fig. S8. ECSA-normalized polarization curves of Co_9S_8@NiFe LDH, Co_9S_8 and NiFe LDH in 1 M KOH.

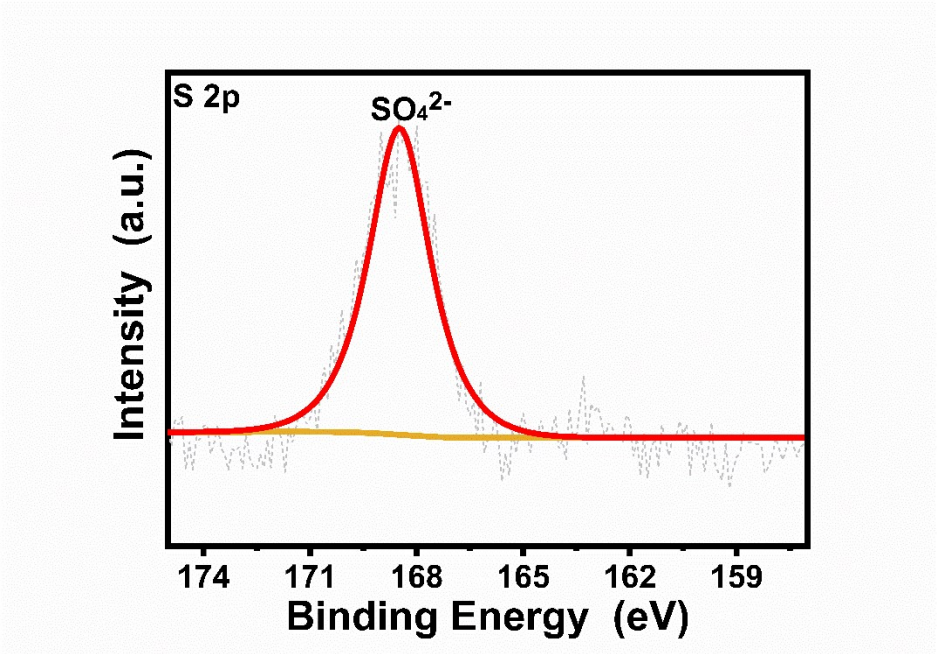

Fig. S9. High-resolution XPS spectrum of S 2p from pristine Co_9S_8 after stability test for OER.

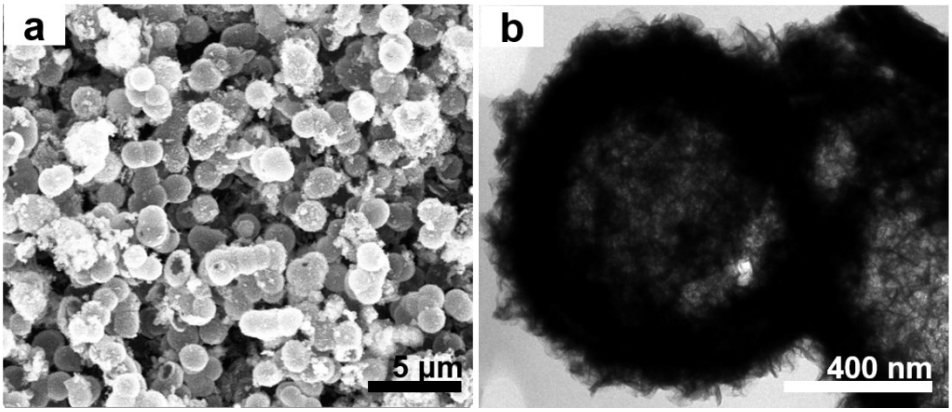

Fig. S10. (a) SEM image and (b) TEM image of pure Co_9S_8 after stability test for OER.

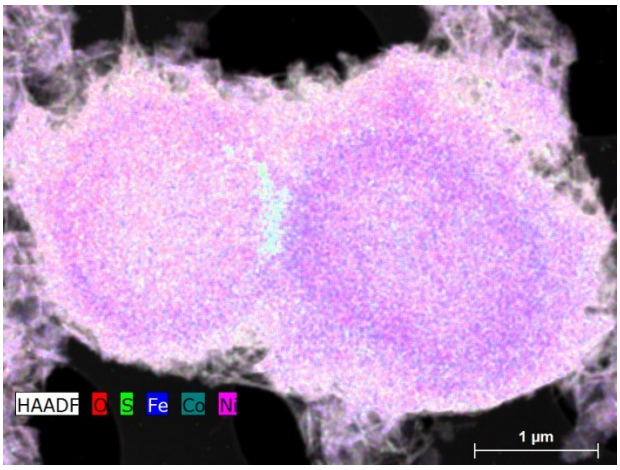

Fig. S11. EDS mapping of Co, S, Ni, Fe and O from Co_9S_8@NiFe LDH after 20-hrs stability test.

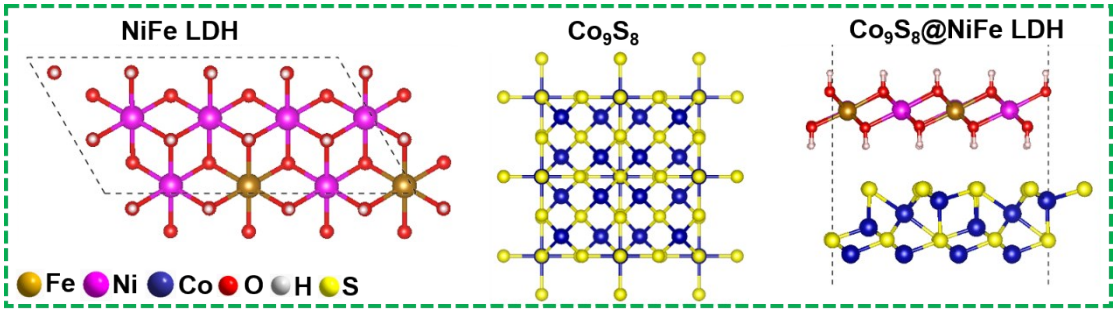

Fig. S12. The optimized crystal structures of NiFe LDH, Co_9S_8 and Co_9S_8@NiFe LDH.

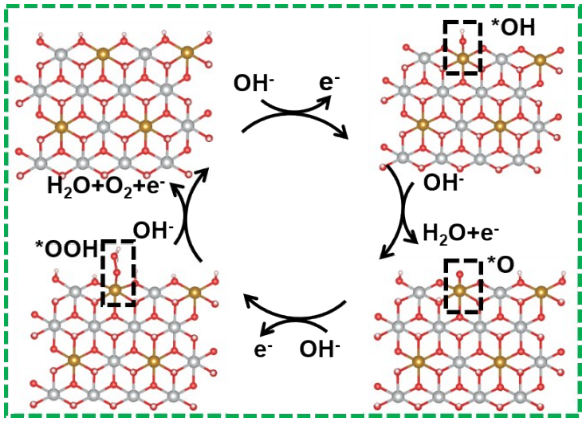

Fig. S13. Schematic illustration of the OER pathway on the NiFe LDH.

Table S1. Comparison of OER activity of Co_9S_8@NiFe LDH with catalysts in previous literatures.

Catalyst	Overpotential (mV) j=10 mA cm^{-2}	Tafel slope	Refs.
Co_9S_8@NiFe LDH	**220**	**52.0**	**This work**
Co_9S_8@NiCo LDH on nickel foam (NF)[9]	278[a]	83.0	Sci. Bull. 2019
(Co,Ni)Se_2@NiFe LDH hollow nanocages[10]	277	75	ACS Appl. Mater. Interfaces 2019
NiFe LDH nanoplates/N-TiO_2 nanotube[11]	235	48.9	ACS Appl. Energy Mater. 2019
hollow TiO_2@Co_9S_8 core-branch arrays[12]	240	55.0	Adv. Sci. 2018
hollow CeO_x/CoS hybrid nanostructure[13]	269	50.0	Angew. Chem. Int. Ed. 2018
Ni_3S_2/NiS hollow core[14]	298	59.8	ACS Appl. Mater. Interfaces 2019
hierarchical hetero-Ni_3Se_4@NiFe LDH micro/nanosheets[15]	223	55.5	Nanoscale Horiz. 2019
NiO@NiFe-LDH on NF[16]	265	72.0	ACS Sustain. Chem. Eng. 2019
N,S-rGO/WSe_2/NiFe-LDH[17]	250	86.0	ACS Appl. Mater. Interfaces 2017
Ag_2S-CoS hetero-nanowires[18]	275	77.1	Catal. Commun. 2019

Co_9S_8 hollow microplates[19]	278	53.0	ACS Appl. Mater. Interfaces 2017
Cobalt sulfide nanosheets[20]	312	69.0	ACS Appl. Energy Mater. 2019
$CuCo_2S_4$ nanosheets[21]	310	86.0	ACS Catal. 2017
$(NiFe)S_2$ nanoparticles grown on graphene[22]	320	61.0	Electrochim. Acta 2018
Graphdiyne@NiFe LDH composite[23]	260	95.0	ACS Appl. Mater. Interfaces 2019
Ball-milled NiFe-LDH[24]	270	36.2	Angew. Chem. Int. Ed. 2019
Ni-Fe LDH hollow nanoprism[25]	280	49.4	Angew. Chem. Int. Ed. 2018
Single-layer NiFe LDH nanosheets[26]	300	40.0	Nat. Commun. 2014

a: an overpotential at the current density of 30 mA cm^{-2}

Table S2. Simulated elemental values of the fitted equivalent circuit corresponding to the EIS spectra in Fig. 3e.

	Co_9S_8@NiFe LDH	Co_9S_8	NiFe LDH
R_s/Ω	0.70	0.68	0.81
R_{ct}/Ω	5.87	7.24	9.96

REFERENCES

1 J. Rossmeisl, Z.-W. Qu, H. Zhu, G.-J. Kroes, J.K. Nørskov, *J. Electroanal. Chem*., 2007, **607**, 83-89.

2 A.V. ´s, Z.-W. Qu, G.-J. Kroes, *J. Phys. Chem. C*, 2008, **112**, 9872–9879.

3 I.C. Man, H.-Y. Su, F. Calle-Vallejo, H.A. Hansen, J.I. Martnez, N.G. Inoglu, J. Kitchin, T.F. Jaramillo, J.K. Nørskov, J. Rossmeisl, *ChemCatChem*, 2011, **3**, 1159-1165.

4 CRC Handbook of Chemistry and Physics, 84th Edition, *J. Am. Chem. Soc*. 2004, **126**.

5 C.-Z. Yuan, Z.-T. Sun, Y.-F. Jiang, Z.-K. Yang, Nan Jiang, Z.-W. Zhao, U.Y. Qazi, W.-H. Zhang, A.-W. Xu, *Small*, 2017, **13**, 1604161.

6 S. Lee, L. Bai, X. Hu, *Angew. Chem. Int. Ed*., 2020, **59**, 8072-8077.

7 S. Lee, K. Banjac, M. Lingenfelder, X Hu, *Angew. Chem. Int. Ed*., 2019, **58**, 10295-10299.

8 R. Subbaraman, D. Tripkovic, K. Chang, D. Strmcnik, A. P. Paulikas, P. Hirunsit, M. Chan, J. Greeley, V. Stamenkovic, N. M. Markovic, *Nat. Mater*., 2012, **11**, 550-557.

9 J. Yan, L. Chen, X. Liang, *Sci. Bull*., 2019, **64**, 158–165.

10 J.G. Li, H. Sun, L. Lv, Z. Li, X. Ao, C. Xu, Y. Li, C. Wang, *ACS Appl. Mater. Interfaces*, 2019, **11**, 8106-8114.

11 X. Liu, Z. Chen, M. Cao, *ACS Appl. Energy Mater*., 2019, **2**, 5960-5967.

12 S. Deng, Y. Zhong, Y. Zeng, Y. Wang, X. Wang, X. Lu, X. Xia, J. Tu, *Adv. Sci*., 2018, 5, 1700772.

13 H. Xu, J. Cao, C. Shan, B. Wang, P. Xi, W. Liu, Y. Tang, *Angew Chem. Int. Ed. Engl*. 2018, **57**, 8654-8658.

14 J. Wang, H.C. Zeng, *ACS Appl. Mater. Interfaces*, 2019, **11**, 23180-23191.

15 T. Zhang, L. Hang, Y. Sun, D. Men, X. Li, L. Wen, X. Lyu, Y. Li, *Nanoscale Horiz*., 2019, **4**, 1132-1138.

16 S. Sirisomboonchai, S. Li, A. Yoshida, X. Li, C. Samart, A. Abudula, G. Guan, *ACS Sustain. Chem. Eng*., 2018, **7**, 2327-2334.

17 X. Xu, H. Chu, Z. Zhang, P. Dong, R. Baines, P.M. Ajayan, J. Shen, M. Ye, *ACS Appl. Mater. Interfaces*, 2017, **9**, 32756-32766.

18 C. Lee, C. Lee, K. Shin, T. Song, H.Y. Jeong, D.Y. Jeon, H.M. Lee, *Catal. Commun*., 2019, **129**, 105749.

19 H. Liu, F.X. Ma, C.Y. Xu, L. Yang, Y. Du, P.P. Wang, S. Yang, L. Zhen, *ACS Appl. Mater. Interfaces*, 2017, **9**, 11634-11641.

20 S. Ju, Y. Liu, H. Chen, F. Tan, A. Yuan, X. Li, G. Zhu, *ACS Appl. Energy Mater*., 2019, **2**, 4439-4449.

21 M. Chauhan, K.P. Reddy, C.S. Gopinath, S. Deka, *ACS Catal.*, 2017, **7**, 5871-5879.

22 C. Liu, H. Ma, M. Yuan, Z. Yu, J. Li, K. Shi, Z. Liang, Y. Yang, T. Zhu, G. Sun, H. Li, S. Ma, *Electrochim. Acta*, 2018, **286**, 195-204.

23 G. Shi, C. Yu, Z. Fan, J. Li, M. Yuan, *ACS Appl. Mater. Interfaces*, 2019, **11**, 2662-2669.

24 D. Zhou, S. Wang, Y. Jia, X. Xiong, H. Yang, S. Liu, J. Tang, J. Zhang, D. Liu, L. Zheng, Y. Kuang, X. Sun, B. Liu, *Angew Chem Int Ed Engl*, 2019, **58**, 736-740.

25 L. Yu, J.F. Yang, B.Y. Guan, Y. Lu, X.W.D. Lou, *Angew Chem Int Ed Engl,* 2018*,* **57**, 172-176.
26 F. Song, X. Hu, *Nat Commun*., 2014, **5**, 4477.